

Seismic hazards assessment of Kumaun Himalaya and adjacent region

P. N. S. Roy · S. K. Mondal · Mallickarjun Joshi

Received: 21 December 2011 / Accepted: 24 May 2012 / Published online: 21 June 2012
© Springer Science+Business Media B.V. 2012

Abstract The ongoing continent–continent collision between Indian and Eurasian plates houses a seismic gap in the geologically complex and tectonically active central Himalaya. The seismic gap is characterized by unevenly distributed seismicity. The highly complex geology with equally intricate structural elements of Himalaya offers an almost insurmountable challenge to estimating seismogenic hazard using conventional methods of Physics. Here, we apply integrated unconventional hazard mapping approach of the fractal analysis for the past earthquakes and the box counting fractal dimension of structural elements in order to understand the seismogenesis of the region properly. The study area extends from latitude 28°N–33°N and longitude 76°E–81°E has been divided into twenty-five blocks, and the capacity fractal dimension (D_0) of each block has been calculated using the fractal box counting technique. The study of entire blocks reveal that four blocks are having very low value of D_0 (0.536, 0.550, 0.619 and 0.678). Among these four blocks two are characterized by intense clustering of earthquakes indicated by low value of correlation fractal dimension (D_c) (0.245, 0.836 and 0.946). Further, these two blocks are categorized as highly stressed zones and the remaining two are characterized by intense clustering of structural elements in the study area. Based on the above observations, integrated analysis of the D_c of earthquakes and D_0 of structural elements has led to the identification of diagnostic seismic hazard pattern for the four blocks.

Keywords Seismicity · Fractal correlation dimension · Capacity fractal dimension and seismic hazard

P. N. S. Roy (✉) · S. K. Mondal
Department of Applied Geophysics, Indian School of Mines, Dhanbad 826004, Jharkhand, India
e-mail: pns_may1@yahoo.com

S. K. Mondal
e-mail: sarojbum@gmail.com

M. Joshi
Department of Geology, Faculty of Science, Banaras Hindu University, Varanasi, India
e-mail: m_joshi@sify.com

1 Introduction

Himalaya is among the most earthquake prone areas of the world. The main seismogenic zones are associated with the collision plate boundary between the Indian and Eurasian plates. Any earthquake study is primarily aimed at reviewing the seismic hazard in a region and mitigating the risk by taking into account the possibilities of future earthquake occurrences. This requires an understanding of the processes related to repeated earthquake occurrences on various seismogenic structures (Gahalaut and Kundu 2011). Based on this context, the relationship between the distribution of structural elements of the region and the past earthquakes has been addressed in this paper. This study can broadly be classified into two categories. The first category deals with the correlation between the past events and examining the fractal correlation dimension (D_c) using correlation integral approach (Grassberger and Procaccia 1983a; Hilarov 1998; Roy and Ram 2006), while the other category deals with the distribution of structural elements (faults, thrusts, lineaments, etc.) and calculation of box counting fractal dimension or capacity fractal dimension (D_0) (Korvin 1992; Turcotte 1997 and Ram and Roy 2005). Thus, integrated results of both categories have significant implications on the seismic hazard assessment for this geologically and tectonically complex region. The Himalayan Range with the largest concentration of mass on earth is characterized by very complex structural elements that play a vital role in determining the seismicity of the region in response to the northward movement of the Indian Plate impinging on Asian mainland. The area of interest for this paper is part of the central seismic gap, lying between the 1905 Kangra and the 1934 Bihar–Nepal earthquake area. This region has not experienced a large earthquake for quite a long time, and the study for hazard mitigation becomes crucial for such a region. Scores of scientific investigations suggest impending large earthquake in future in this zone. Several researchers like (Khattri and Tyagi 1983; Khattri 1987, 1995; Bilham et al. 1995; Mukhopadhyay et al. 2004; Jouanne et al. 2004; Singh et al. 2010) emphasize the possibility of large future earthquakes in this very zone. The seismicity of a region is dictated by the interaction between subsurface geology and regional active tectonics of that region. A seismic tremor can have devastating effects on heavily populated areas and may lead to a serious hazard in that region. The study area is inhabited and dotted with many densely populated towns with people living both on mountains and their foothills. As the area houses a large number of structures including buildings, dams, and bridges, the consequences of an earthquake get multiplied manifolds. The damage threat due to a possible earthquake is more serious due to the effects of triggered landslides on the viable motor road. Thus, the seismic hazard estimation for the region is an imperative need for the safety and security of these mountain dwellers living under the constant threat of a major earthquake. It is in this backdrop that the geology and seismicity of the region in and around the study area need to be investigated in details. Major structural and tectonic elements exposed in and around the region are Indus Suture, Karakoram Fault, Main Central Thrust (MCT), Main Boundary Thrust (MBT), Main Frontal Thrust (MFT), Jwala Mukhi Thrust, Drang Thrust, Sundar Nagar Fault, Kaurik Fault system, Alaknanda Fault, Martoli Thrust, Mahendragarh Dehradun Fault, North Ramgarh Thrust, South Ramgarh Thrust, South Almora Thrust, North Almora Thrust, Moradabad Fault, and Great Boundary Fault (Joshi 1999; Dasgupta et al. 2000). The region is seismologically one of the most active zones of the Himalayan terrain. Our analysis effectively brings out that some parts of the study area are threatened by high seismic risk. Our unconventional hazard mapping approach is mainly using correlation fractal dimension for understanding the pattern of earthquake occurrence and the use of

capacity fractal dimension to quantify the distribution of structural elements of the region.

The fault system is analyzed with the help of the box counting method, which is a popular tool of fractal analysis. This method was earlier used by Hirata (1989a) for fault systems in Japan; by Idziak and Teper (1996) to study fractal dimensions of fault networks in the upper Silesian coal basin, Poland; Angulo-Brown et al. (1998) studied the distribution of faults, fractures, and lineaments over a region on the western coast of the Guemero state in southern Mexico. A similar technique was used by Okubo and Aki (1987) to study the fractal geometry of the San Andreas fault system; by Sukmono et al. (1994, 1997) to study the fractal geometry of the Sumatra fault system. Sunmonu and Dimri (2000) studied the fractal geometry and seismicity of Koyna–Warna, India, by using the same technique. Ram and Roy (2005) used the technique for the Bhuj Earthquake analysis. Thingbaijam et al. (2008) applied the method for the determination of capacity dimension (D_0) for the fault system. Gonzato et al. (1998) and Gonzato (1998) have developed computer programs to evaluate fractal dimension through the box counting method, which potentially solves the problem of the process of counting. The main disadvantage of the program is that it deals directly with the images. Joshi and Rai (2003a) used fractal geometry for appraisal of inverted Himalayan metamorphism, and Joshi and Rai (2003b) demonstrated fractal dimension as a new measure of neotectonics activity. The technique has also been widely used in various fields for characterization of specific mineral occurrence in nature. Recently, researchers (Ford and Blenkinsop 2008; Raines 2008; Carranza 2008, 2009) applied the same method in order to characterize spatial pattern of occurrences of mineral deposits. Chauveau et al. (2010) used capacity dimension and correlation dimension for the study of color images.

2 Methodology

2.1 Correlation dimension

A fractal dimension is a sophisticated statistical tool to quantify the dimensional distribution of seismicity or structural elements, its randomness, and characterization (e.g., Kagan and Knopoff 1980; Ogata 1988; Hirata 1989b). The fractal dimension may be used as a quantitative measure of the degree of heterogeneity of seismic activity in faults system of a region (Oncel et al. 1996). Therefore, it gives vital information about the stability of a region. A change in the fractal dimension corresponds to the dynamic evolution of the states of the system. The fractal dimension, D_c value, is estimated using the correlation dimension. The correlation dimension as defined by Grassberger and Procaccia (1983b) measures the spacing of a set of points, which in this case are the earthquake epicenters. The correlation integral technique that gives the correlation dimension is preferable because of its greater reliability and sensitivity to small changes in clustering properties (Kagan and Knopoff 1980; Hirata 1989b).

The fractal correlation dimension is derived from the correlation integral (Grassberger and Procaccia 1983a; Hilarov 1998; Roy and Ram 2006; Roy and Nath 2007; Roy and

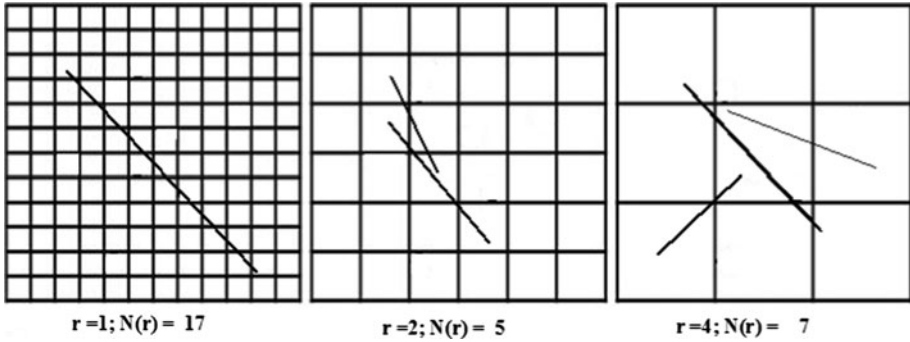


Fig. 1 A schematic diagram of the *box counting* method for measuring the fractal dimension of the fault system. The r is measure of side of a *square box*, and $N(r)$ is number of *boxes* containing at least one or any part of fault system

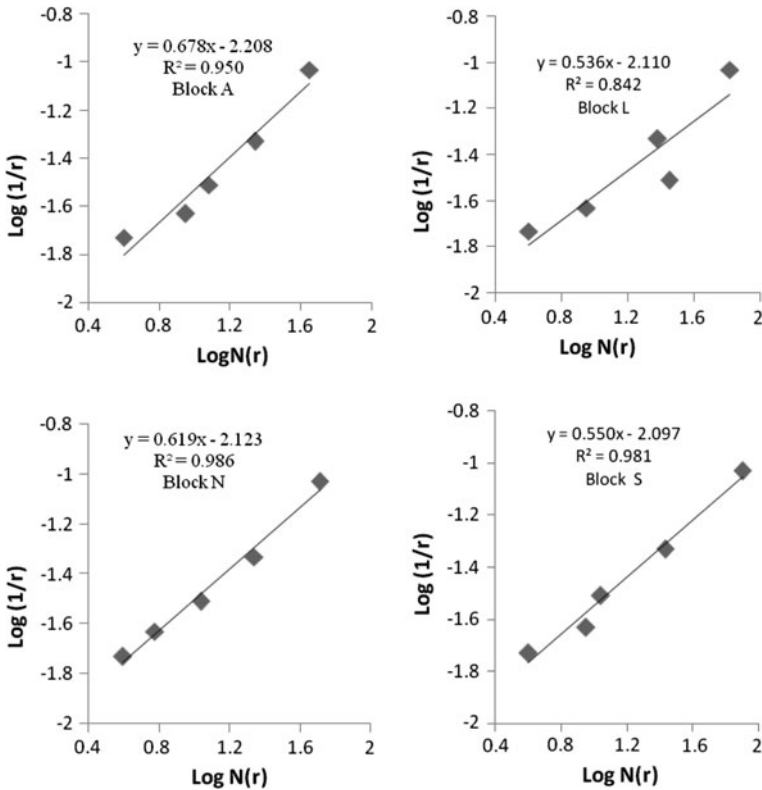


Fig. 2 The $\log (1/r)$ versus $\log N(r)$ is shown for the determination of capacity dimension of the block “A,” “N,” “L,” and “S”. The slope of the line assigns the value of capacity dimension. R^2 represents correlation coefficients of the regression line

Padhi 2007; Singh et al. 2009; Roy and Mondal 2009), which is a cumulative correlation function that measures the fraction of points in the two-dimensional space and is defined as:

$$C(r) = \frac{2}{N(N-1)} \sum_{j=1}^N \sum_{i=j+1}^N H(r - r_{ij}) \tag{1a}$$

$$r = \cos^{-1}(\cos \theta_1 \cos \theta_2 + \sin \theta_1 \sin \theta_2 \cos(\phi_1 - \phi_2)) \tag{1b}$$

where N (for 50 events windows, N will be $^{50}C_2$, that is, 1225) is the total number of pairs in the fractal set to determine D_c , r is the length scale, r_{ij} the distances between the points of a set, which are obtained through spherical triangle method (Eq. 1b), where r the angular distance between two events, $(\theta_1, \phi_1), (\theta_2, \phi_2)$ are colatitudes and longitudes, respectively, of two events, H is the Heaviside step function. Therefore, $C(r)$ is proportional to the number of pairs of points of the fractal set separated by a distance less than r . If the system of points examined is a fractal set, the graph of $C(r)$ in logarithmic coordinates must be a linear function with slope D_c equal to the fractal dimension of the system. The D_c value is inversely related to the degree of clustering and it requires higher degree of accuracy in both space and time of occurrence of events as the present analysis depends on the spatiotemporal distribution of earthquake sequences. Lower the value of D_c higher the clustering (Hirata et al. 1987; Kagan et al. 2006) of events and vice versa occurs in the study zone. This is exercised considering 50 events windows to depict the variation in D_c with time.

2.2 Fractals in geological structural system

A fractal distribution requires that the number of objects larger than a specified size has a power-law dependence on the size:

$$N(r) \propto 1/r, \tag{2}$$

where $N(r)$ is the number of objects (i.e., fragments) with a characteristic linear dimension r (specified size). Equation (2) can be written as:

$$N(r) = c/r^{D_0}, \tag{3}$$

where c is the constant of proportion and D_0 is the fractal dimension that gives $N(r)$ a finite value; otherwise, with the decrease in size r in Eq. (2), the value would have reached infinite. For box counting, $N(r)$ represents the number of occupied boxes and r is the length of the box side. Hirata 1989a used box counting (e.g., Turcotte 1989, 1997) to cover the fault traces.

The fractal dimension of the fault system can be measured by the box counting method (Fig. 1). The procedure is repeated for different values of r , and the results are plotted in a log–log graph. The slope of the line assigns the value of capacity dimension (Preuss 1995; Turcotte 1997; Ram and Roy 2005) as depicted in Fig. 2. If the fault system under investigation is a fractal, the plots of $N(r)$ versus r can be described by a power-law function (Mandelbrot 1985; Feder 1988) as in Eq. (3). The relation in Eq. (3) can be represented as a linear function in a log–log graph:

$$\text{Log } N(r) = \text{log } c - D_0 \text{log } r, \tag{4a}$$

where c is the constant of proportion, and the slope, D_0 , of the linear log–log plots of $N(r)$ versus r represents a measure of the fractal dimension of the system. In this method, the faults and other structural elements on the map were initially superimposed on a square grid size s_0 . The unit square s_0^2 was sequentially divided into small squares of size

$s_1 = s_1^x/2, s_0/4, s_0/8, \dots$. The number of squares or boxes $N(s_i)$ intersected by at least one fault line is counted each time. If the fault system is a self-similar structure, then following Mandelbrot (1983), $N(s_i)$ is given by:

$$N(s_i) \sim (s_0/s_i)^{D_0} \sim s_i^{-D_0}, \quad (4b)$$

where D_0 is interpreted as the fractal dimension of the fault system. The fractal dimension D_0 was determined from the slope of the $\log N(s_i)$ versus $\log(s_0/s_i)$ line of the data points obtained by counting the number of boxes covering the curve and the reciprocal of the scale of the boxes.

The area of the present study covers the belt between latitude 28°N–33°N and longitude 76°E–81°E, and it was divided into twenty-five blocks (Fig. 3). Surface and volume fractal dimensions were obtained for blocks (A–Y) separately shown in Table 1. The four blocks denoted in bold (i.e. A, L, N & S) are the identified possible high seismic risk zone. On the other hand the fault line in block “Y” is not fractal. Box counting dimension for each block marked by capital letters (A–Y) is given in Table 1. The volume fractal dimension is equal to one plus surface fractal dimension (Turcotte 1997; Maus and Dimri 1994; Sunmonu and Dimri 2000). Usually, the surface exposed faults are the two-dimensional expression of embedded faults in the three-dimensional volume mass. Hence, volume fractal dimension will give the perspective of understanding the three-dimensional heterogeneity of the complex Himalayan structure. The geological elements have been taken from Dasgupta et al. (2000). Each block is of the order of 1° × 1° on the maps.

3 Data used

The USGS PDE data ($m_b \geq 3.5$) have been used for the period 1973–2008 and Wadia Institute of Himalayan Geology local network data ($m_b \geq 1.2$) for the period of 2004 to 2006 for the study of region in search of seismicity patterns of the region. Further, considering the catalogue of USGS PDE for the entire period from 1973 to 2008, we felt that the local earthquakes recorded by the Wadia Institute of Himalayan Geology (WIHG) will give better idea about the stress pattern. As earthquake scaling and frequency of occurrence relations require that small earthquakes be just as important as larger ones in redistributing the forces that drive relative displacements across active faults of any dimension, including plate boundaries. The removal of data set recorded by local networks will lead to decrease in a good chunk of data, which would have played a very important role in deciding the energy buildup in the system in the lookout of the zone of extreme stress buildup as a slow process for nucleating a strong event. However, the Gutenberg–Richter relation is not used directly in the present analysis where b value is not a parameter considered in relation to D_c . Moreover, our prime goal here is to find the D_0 for structural elements to get the seismotectonic of the region and to also see the relation with D_c , whereas correlation of such different parameters is new of its kind in this seismic hazard analysis. The completeness magnitude is not expected to change the correlation dimension formulation in the search of low D_c . Even Oncel and Wilson (2002, 2006); Nakaya and Hashimoto (2002); Roy and Ram (2006) did not specify completeness in their studies. The tectonic features of the region have been utilized from Dasgupta et al. (2000) for capacity dimension determination. In the determination of D_0 , care has been taken in all respect. Figure 3 shows the utilized structural elements for the box counting dimension. The area covers from latitude 28°N–33°N and longitude 76°E–81°E. Figure 3 shows the distribution of structural

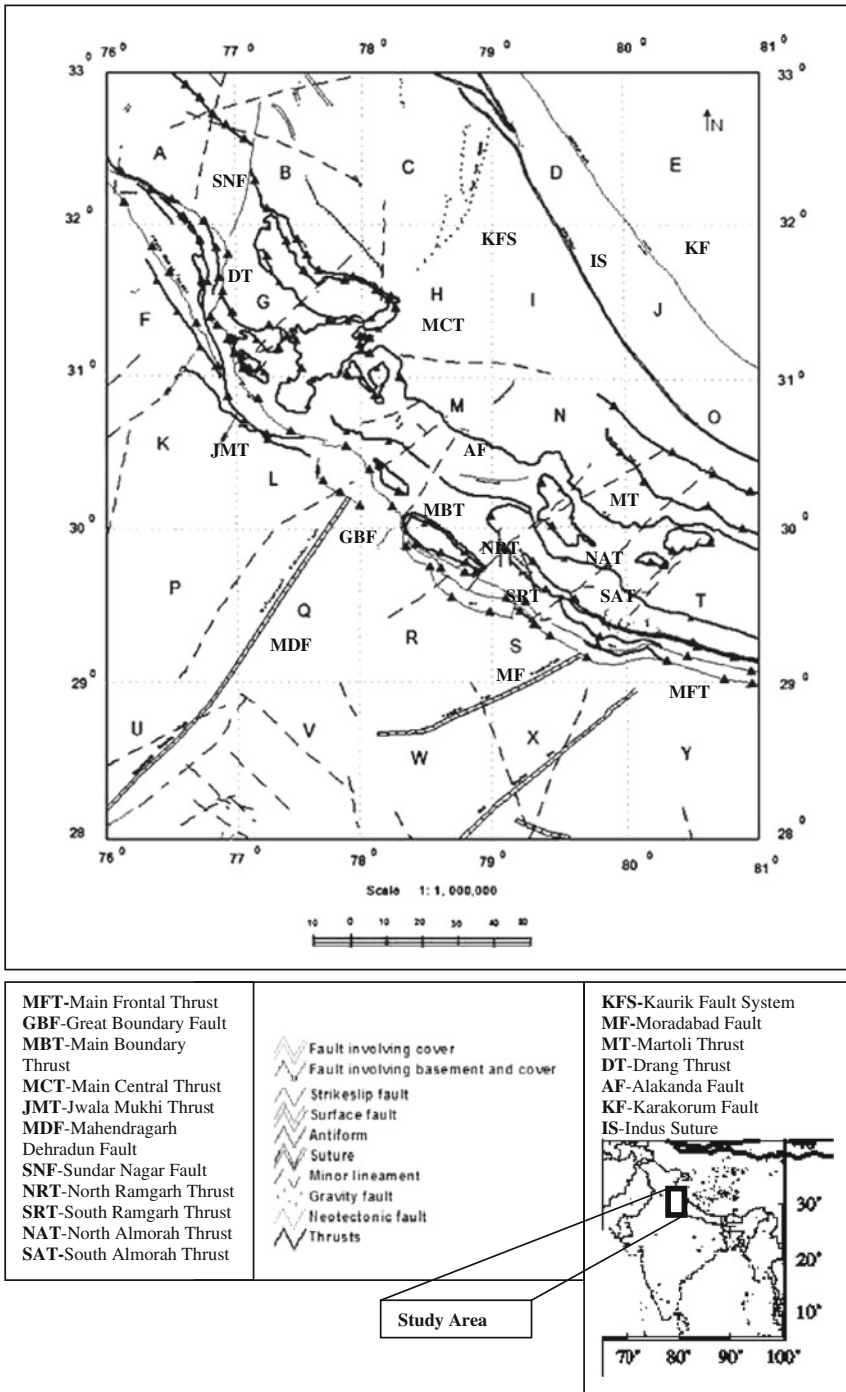


Fig. 3 The map of the region shows the tectonic features of the entire study area used for the determination of capacity fractal dimension (D_0) (Modified after Dasgupta et al. 2000)

Table 1 Box counting dimension and volume fractal dimension for twenty-five blocks, where R^2 represents the regression coefficient for straight line fit to obtain box counting fractal dimension

Serial/ block no.	Latitude–longitude of the sub area in $1^\circ \times 1^\circ$	Box counting fractal dimension (D_0)	R^2 (regression coefficient)	Volume fractal dimension = $D_0 + 1$
A	32°N–33°N 76°E–77°E	0.678	0.950	1.678
B	32°N–33°N 77°E–78°E	0.629	0.982	1.629
C	32°N–33°N 78°E–79°E	0.793	0.990	1.793
D	32°N–33°N 79°E–80°E	0.824	0.960	1.824
E	32°N–33°N 80°E–81°E	No structural element exists	–	–
F	31°N–32°N 76°E–77°E	0.619	0.974	1.619
G	31°N–32°N 77°E–78°E	0.574	0.978	1.574
H	31°N–32°N 78°E–79°E	0.721	0.996	1.721
I	31°N–32°N 79°E–80°E	1.043	0.995	2.043
J	31°N–32°N 80°E–81°E	0.793	0.980	1.793
K	30°N–31°N 76°E–77°E	0.805	0.993	1.805
L	30°N–31°N 77°E–78°E	0.536	0.842	1.536
M	30°N–31°N 78°E–79°E	0.575	0.991	1.575
N	30°N–31°N 79°E–80°E	0.619	0.986	1.619
O	30°N–31°N 80°E–81°E	0.608	0.979	1.608
P	29°N–30°N 76°E–77°E	1.231	0.949	2.231
Q	29°N–30°N 77°E–78°E	0.776	0.958	1.776
R	29°N–30°N 78°E–79°E	0.652	0.968	1.652
S	29°N–30°N 79°E–80°E	0.550	0.981	1.550
T	29°N–30°N 80°E–81°E	0.570	0.980	1.570
U	28°N–29°N 76°E–77°E	0.564	0.984	1.564
V	28°N–29°N 77°E–78°E	0.674	0.986	1.674
W	28°N–29°N 78°E–79°E	0.868	0.976	1.868
X	28°N–29°N 79°E–80°E	0.683	0.990	1.683
Y	28°N–29°N 80°E–81°E	Not Fractal	–	–

elements in the entire study area that has been divided into twenty-five blocks as marked by capital letters (A to Y). The corresponding box counting fractal dimensional value is depicted in Table 1. The variation in capacity dimension of each block may be related to the physical clustering and distribution of the fault system.

4 Results and discussion

The fractal dimension of past earthquakes occurrence was first determined to observe the variation in D_c value with time. High seismic activity and the clustering of the area are determined with the significant low value of D_c . The D_c value was calculated for using fifty events consecutive windows of the data set as its variation shown in the Table 2. Further, D_c value is inversely related to degree of clustering of events (Kagan et al. 2006; Roy and Padhi 2007; Thingbaijam et al. 2008). Hence, low D_c value indicates high clustering (Hirata et al. 1987) of earthquakes occurrence. This helps in the identification of highly clustered zone as indicated in Fig. 4a–c. One strong event has occurred in the sixth window

Table 2 Here, the variation in D_c value for fifty events windows with mean time is shown. The three low D_c values are marked in bold where one window has one strong earthquake and other two windows have no such events

Serial no.	Mean time (t) of each fifty events windows (in months/remarks)	D_c
1	26.11	1.615
2	72.74	1.522
3	148.44	1.824
4	214.58	1.431
5	264.77	1.546
6	308.21 (6.6Ms, 28.03.99)	0.836
7	342.25	1.295
8	372.28	1.280
9	389.029 (LOW D_c, 28.12.04)	0.946
10	391.29 (LOW D_c, 01.03.05)	0.285
11	392.73	1.346
12	395.54	1.253
13	401.04	1.263
14	405.98	1.579
15	412.87	1.447
16	426.47	1.192

(Table 2) of magnitude 6.6 Ms, but the other two low D_c value windows (i.e., 9th and 10th) have no such strong events, showing the present activity for future strong event.

The three-dimensional map of volume fractal dimension distribution of the entire study area is depicted in Fig. 5 as calculated and shown in Table 1. Lower volume fractal dimension distribution is observed along MBT. On the other hand, there exists a gradual increase in volume fractal distribution through MBT toward Main Central Thrust (MCT). Higher volume fractal dimension distribution is along Indus Suture and Karakoram Fault (Fig. 5). Hence, higher volume fractal dimension gives the view of understanding the three-dimensional heterogeneity of the complex Himalayan structure, which is predominant in the above two regions like Indus Suture and Karakoram as well as for the region near MCT as shown in the Fig. 3. Here, the volume fractal dimension of structural elements present in each block was calculated using the box counting technique (Carlson 1991; Hodkiewicz et al. 2005; Ram and Roy 2005; Ford and Blenkinsop 2008; Raines 2008; Carranza 2008, 2009).

The surface fractal dimension quantifies the geometrical distribution of fault system, which is the quantitative fractal analysis of complex tectonics governing seismic activity in the region. The results show some boxes are having lowest D_0 values. The estimated D_0 is found to vary from 0.536 to 1.231. The block “L” has the lowest capacity dimension, and block “P” has the highest D_0 value (Fig. 5). The block “L” has a system of faults well distributed in the region. On the other hand, block “P” has only one fault line. So the physical significance of low and high D_0 may be understood well with capacity dimension. A value close to 2 suggests that it is a plane that is filled up by structural elements, while a value close to 1 implies that line sources are predominant (Aki 1981). In our study region, none of the blocks have a value of 1 or 2.

The analysis for the entire region gives insights about the seismic hazard prevalent in and around the four blocks. The three lowest D_c earthquakes distribution of fifty events

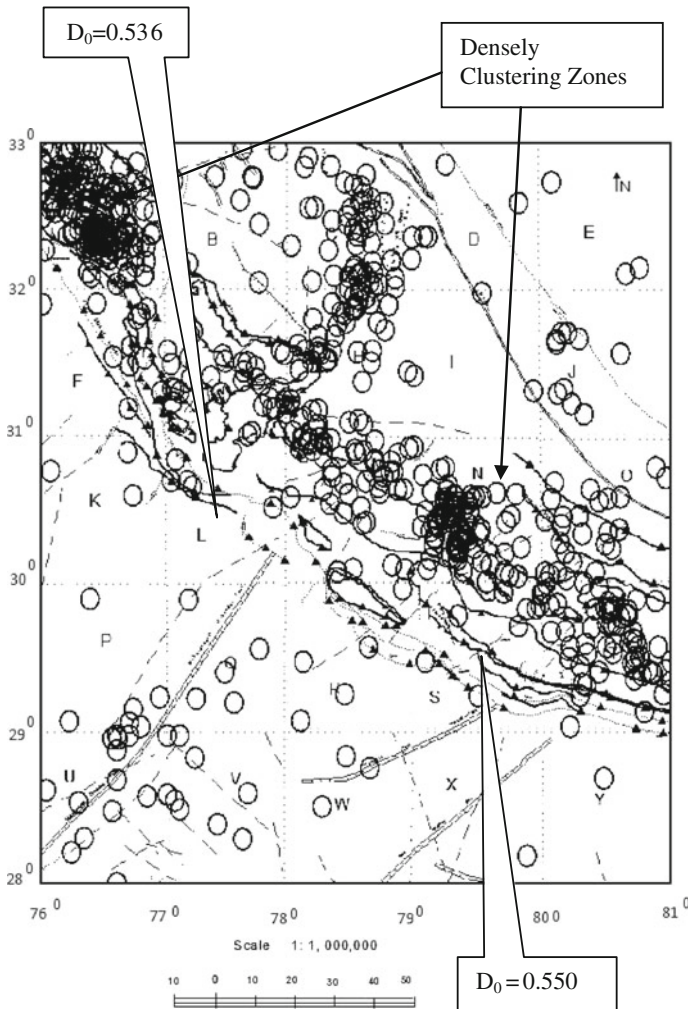


Fig. 4 **a** Events distribution showing two zones one at latitude 32°N–33°N and longitude 76°E–77°E and other at latitude 30°N–31°N and longitude 79°E–80°E where intense seismicity is observed. The two values 0.536 and 0.550 are the lowest capacity dimension. **b** Events distribution of three low D_c of fifty events windows showing the intense seismicity clustering at two zones lying at latitude 32°N–33°N and longitude 76°E–77°E and latitude 30°N–31°N and longitude 79°E–80°E, where low capacity dimension of structural elements is also observed. **c** The block marked by capital letters A, L, N, and S is estimated as possible high seismic zones of the study area

windows clearly indicates the intense clustering of events in blocks “A” and “N” (Fig. 4a, b). The reason may be the low capacity dimension value of 0.678 and 0.619 for the fault systems, respectively. The tectonic elements in blocks “A” and “N” may be the cause of occurrence of higher intensity earthquakes. The present seismic activity scenario in the region may be supported by the existence of complex fault system and its relation (Fig. 4a–c). The structural elements in these two blocks are Drang Thrust, Minor Lineament, part of Jwalamukhi Thrust, Anti-form, Neotectonic fault Thrust, Main Central Thrust, Minor Lineament, Faults, Alaknanda Faults, Martoli Thrust, etc. On the other hand, two blocks

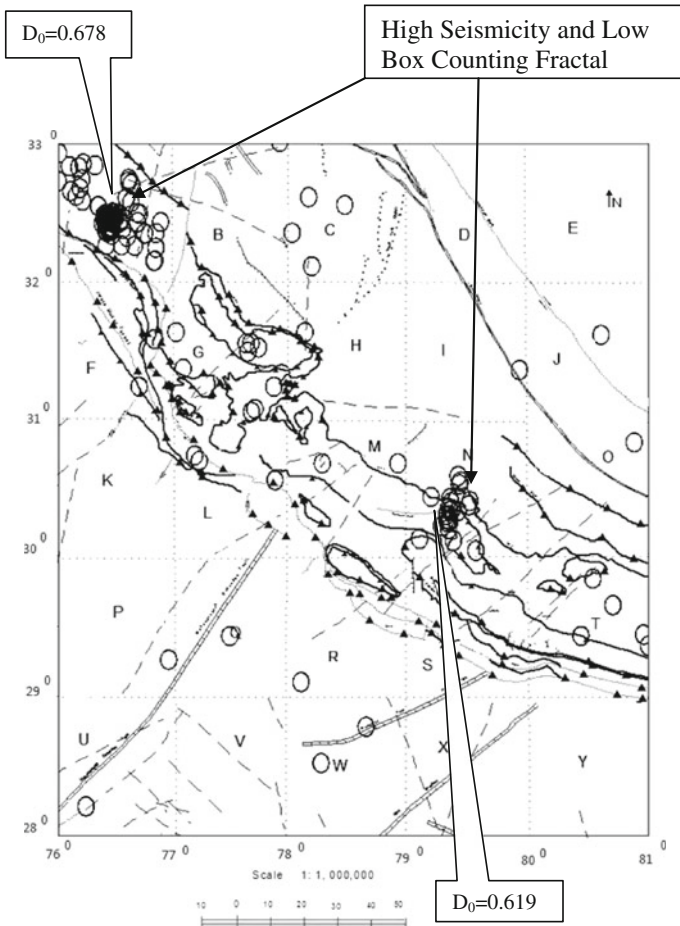


Fig. 4 continued

“L” and “S” with lowest D_0 value (0.536, 0.550) are experiencing very little seismic activity in comparison with the blocks “G,” “M,” “T,” and “U” despite the low value of D_0 (0.574, 0.575, 0.570, and 0.560, respectively, Fig. 3 and Table 1). The smaller magnitude earthquakes are not occurring in blocks “L” and “S”. Hence, the release of energy is not taking place in blocks L and S. These zones may be considered as the high seismic zones of the study area. The important tectonic elements of these blocks are Moradabad Fault, South Ramgarh Thrust, North Ramgarh Thrust, North Almora Thrust, South Almora Thrust, MBT, Minor Lineament, Faults, Neotectonic Fault and Mahendragarh Dehradun Fault, etc.

5 Conclusions

In our effort to delineate the high seismicity zone and consequent seismic hazards, an investigation for D_0 of structural elements and D_c of earthquakes occurrence was

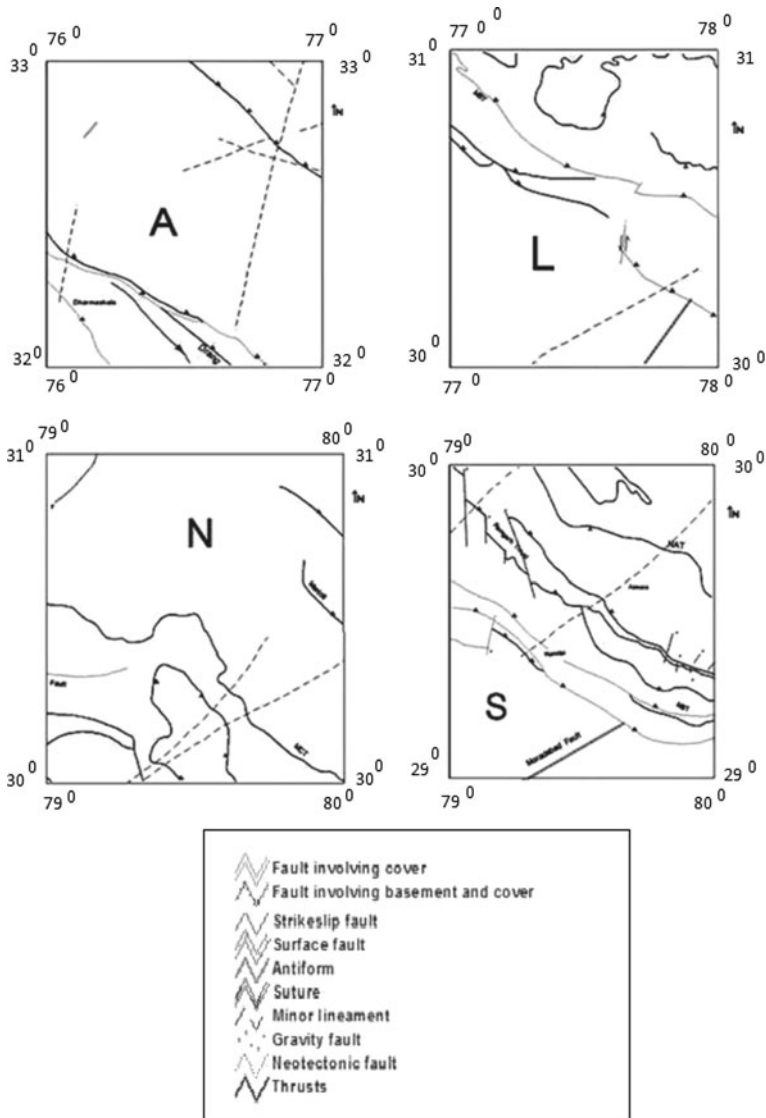


Fig. 4 continued

undertaken. The study of Kumaun Himalaya and adjacent region leads to the understanding of the D_c value fluctuations. The D_c value for 50 events windows analysis carried out for the entire study area, helped in the identification of intense seismicity with low values. The identified decrease in D_c value is the zone of highly clustered seismicity. The decrease in this D_c value can be considered as an indicator for a future strong event. The significant low D_c value represents the possible rupture nucleation point or highly stressed region and shows clustering of the events as indicated in Fig. 4a, b. The correlation dimension (D_c) considered in the present study depicts intense clustering at two zones as shown in Fig. 4a, b.

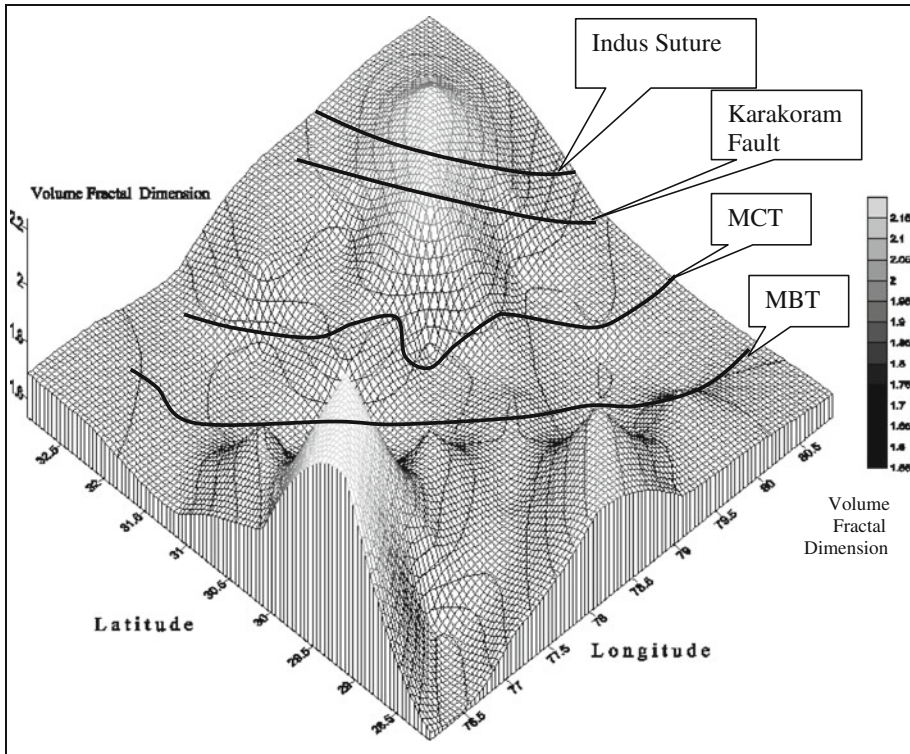


Fig. 5 The figure shows the map of the volume fractal dimension distribution of the studied area

Moreover, D_0 analysis for the tectonic elements of the study region helped in demarcating two blocks (i) with latitude 32°N – 33°N ; longitude 76°E – 77°E , that is, block “A” and (ii) with latitude 30°N – 31°N ; longitude 79°E – 80°E , that is, block “N,” which are having low D_0 and also corresponding low correlation fractal dimension value of high seismic activity obtained for the same zones. Hence, these blocks and their surroundings may be considered as a high risk zone. On the other hand, the blocks “L” and “S” with lowest D_0 and having lesser seismicity in comparison with the other four blocks “G”, “M”, “T,” and “U” are considered as the highest seismic risk zone of the study area (Fig. 4c).

Our correlation integral approach of fractal analysis is of great importance in extracting the highly clustered region of earthquakes in terms of numerical values that can be discriminated with any other region under study area. On the other hand, spatial distribution of earthquakes as a whole will not help in segregating the different zones of highly clustering. In addition to this, the capacity dimension determination of structural elements helped more in identifying the four blocks of high seismic risk zones. Several workers have calculated fractal dimension, but the approach for demarcating the seismic hazard zones has not been applied earlier. Moreover, our prime goal here is to find the D_0 for structural elements to get the seismotectonic of the region and to also see the relation with D_c , whereas correlation of such different parameters is new of its kind in this seismic hazard analysis.

Acknowledgments PNSR and SKM gratefully acknowledge Ministry of Earth Science, Government of India, for sponsoring this work by the project (MoES/P.O.(Seismo)/GPS/60/2006). Wadia Institute of Himalayan Geology is thankfully acknowledged for providing local network data. MJ gratefully acknowledges the facilities rendered by the CAS-I Programme of the UGC and the Head, Department of Geology, Banaras Hindu University. We are very much thankful to anonymous reviewers for their suggestions that improved the manuscript.

References

- Aki K (1981) A probabilistic synthesis of precursor phenomena. In: Simpson DW, Richards PG (eds) Earthquake prediction, Maurice Ewing Series 4, AGU, pp 566–574
- Angulo-Brown F, Ramirez-Guzman AH, Yezpe E, Rudoif-Navarro A, Pavia-Miller CG (1998) Fractal geometry and seismicity in the Mexican subduction zone. *Geofisica Internat* 37:29–33
- Bilham R, Bodin P, Jackson M (1995) Entertaining a great earthquake in Western Nepal: historic inactivity and development of strain. *J Nepal Geol Soc* 11:73–88
- Carlson CA (1991) Spatial distribution of ore deposits. *Geology* 19:111–114
- Carranz EJM (2009) Controls on mineral deposit occurrence inferred from analysis of their spatial pattern and spatial association with geological features. *Ore Geol Rev* 35:383–400
- Carranza EJM (2008) Geochemical anomaly and mineral prospectivity mapping in GIS. *Handbook of exploration and environmental geochemistry*, vol 11. Elsevier, Amsterdam, p 51
- Chauveau J, Rousseau D, Chapeau-Blondeau F (2010) Fractal capacity dimension of three-dimensional histogram from color images. *Multidimens Syst Signal Process* 1:197–211
- Dasgupta S, Pande P, Ganguly D, Iqbal Z, Sanyal K, Venkatraman NV, Dasgupta S, Sural B, Harenranath L, Mazumdar K, Sanyal S, Roy A, Das LK, Misra PS, and Gupta HK (2000) In: Narula PL, Acharyya SK, Banerjee J (eds) *Seismotectonic atlas of India and its environs*. Geological Survey of India
- Feder J (1988) *Fractals*. Plenum, New York, p 283
- Ford A, Blenkinsop TG (2008) Combining fractal analysis of mineral deposit clustering with weights of evidence to evaluate patterns of mineralization: application to copper deposits of the Mount Isa Inlier, NW Queensland, Australia. *Ore Geol Rev* 3:435–450
- Gahalaut VK, Kundu B (2011) Possible influence of subducting ridges on the Himalayan arc and on the ruptures of great and major Himalayan earthquakes. *Gondwana Res* (in press). doi:[10.1016/j.gr.2011.07.021](https://doi.org/10.1016/j.gr.2011.07.021)
- Gonzato G (1998) A practical implementation of the box-counting algorithm. *Comput Geosci* 24:95–100
- Gonzato G, Mulargia F, Marzocchi W (1998) Practical application of fractal analysis: problems and solutions. *Geophys J Int* 132:275–282
- Grassberger P, Procaccia I (1983a) Characterizations of stranger attractors. *Phys Rev Lett* 50:346–349
- Grassberger P, Procaccia I (1983b) Measuring the strangeness of strange attractors. *Physica D* 9:189–208
- Hilarov VL (1998) Self-similar crack-generation effects in the fracture process in brittle materials. Modelling simulation. *Material Sci Eng* 6:337–342
- Hirata T (1989a) Fractal dimension of fault systems in Japan: fractal structure in rock fracture geometry at various scales. *Pure Appl Geophys* 131:157–170
- Hirata T (1989b) A correlation between the b-value and the fractal dimension of earthquakes. *J Geophys Res* 94:7507–7514
- Hirata T, Satoh T, Ito K (1987) Fractal structure of spatial distribution of microfracturing in rock. *Geophys J R Astron Soc* 90:369–374
- Hodkiewicz PF, Weinberg RF, Gardoll SJ, Groves DI (2005) Complexity gradients in the Yilgarn Craton: fundamental controls on crustal-scale fluid flow and formation of world-class orogenic-gold deposits. *Aust J Earth Sci* 52:831–841
- Idziak A, Teper L (1996) Fractal dimension of faults network in the Upper Silesian Coal Basin (Poland): preliminary studies. *Pure Appl Geophys* 147:239–247
- Joshi M (1999) Evolution of the basal shear zone of the Almora Nappe, Kumaun Himalaya, Gondwana Research Group, Geodynamics of NW Himalaya, Japan. *Memoir* 6:69–80
- Joshi M, Rai JK (2003a) An appraisal of models for inverted Himalayan Metamorphism. *Memoir volume. J Geol Soc India* 52:359–380
- Joshi M, Rai JK (2003b) Fractal dimension as a new measure of neotectonic activity in Kakrighat Area, Kumaun Himalaya. *J Geol Soc India* 61:664–672
- Jouanne F, Mugnier JL, Gamond JF, Le Fort P, Pandey MR, Bollinger L, Flouzat M, Avouac JP (2004) Current shortening across the Himalayas of Nepal. *Geophys J Int* 157(1):1–14

- Kagan YY, Knopoff L (1980) Spatial distribution of earthquakes: the two-point correlation function. *Geophys J R Astron Soc* 62:303–320
- Kagan YY, Jackson DD, Rong YF (2006) A new catalogue of southern California earthquakes, 1800–2005. *Seismol Res Lett* 77(1):30–38
- Khattri KN (1987) Great earthquakes, seismicity gaps and potential for earthquake disaster along Himalaya plate boundary. In: Mogi K, Khattri KN (eds) *Earthquake prediction. Tectonophysics*, vol 138, pp 79–92
- Khattri KN (1995) Fractal description of seismicity of India and inference regarding earthquake hazard. *Curr Sci* 69:361–366
- Khattri KN, Tyagi AK (1983) Seismicity patterns in the Himalayan plate boundary and identification of areas of high seismic potential. *Tectonophysics* 96:281–297
- Korvin G (1992) *Fractal models in the earth sciences*. Elsevier, Amsterdam, p 369
- Mandelbrot BB (1983) *The fractal geometry of nature*. Freeman, New York
- Mandelbrot BB (1985) Self-affine fractals and fractal dimension. *Phys Scr* 32:257–260
- Maus S, Dimri VP (1994) Scaling properties of potential fields due to scaling sources. *Geophys Res Lett* 21:891–894
- Mukhopadhyay B, Dasgupta S, Dasgupta S (2004) Clustering of earthquake events in the Himalaya—its relevance to regional tectonic set-up. *Gondwana Res* 7(4):1242–1247
- Nakaya S, Hashimoto T (2002). Temporal variation of multifractal properties of seismicity in the region affected by the mainshock of the October 6, 2000 Western Tottori prefecture, Japan, earthquake ($M = 7.3$). *Geophys Res Lett* 29:133-1–133-4
- Ogata Y (1988) Statistical models for earthquake occurrences. *J Am Stat As* 83:9–27
- Okubo PG, Aki K (1987) Fractal geometry in the San Andreas fault system. *J Geophys Res* 92:345–355
- Oncel AO, Wilson TH (2002) Space-time correlations of seismotectonic parameters: example from Japan and from Turkey preceding the Izmit earthquake. *Bull Seismol Soc Am* 92:339–349
- Oncel AO, Wilson T (2006) Evaluation of earthquake potential along the northern Anatolian Fault zone in the Marmara Sea using comparisons of GPS strain and seismotectonics parameters. *Tectonophysics* 418:205–218
- Oncel AO, Main I, Alptekin O, Cowie P (1996) Temporal variations in the fractal properties of seismicity in the North Antolian fault zone between 31° E and 41° E. *Pure Appl Geophys* 147:147–159
- Preuss SA (1995) Some remarks on the numerical estimation of fractal dimension: In: Ch. Bartone C, La Pointe PR (eds) *Fractals in earth sciences*. Plenum Press, New York, pp 65–76
- Raines GL (2008) Are fractal dimensions of the spatial distribution of mineral deposits meaningful? *Nat Resour Res* 17:87–97
- Ram A, Roy PNS (2005) Fractal dimensions of blocks using a box-counting technique for the 2001 Bhuj Earthquake, Gujarat, India. *Pure Appl Geophys* 162:531–548
- Roy PNS, Mondal SK (2009) Fractal nature of earthquake occurrence in Northwest Himalayan Region. *J Indian Geophys Union* 13(2):63–68
- Roy PNS, Nath SK (2007) Precursory correlation dimensions for three great earthquakes. *Curr Sci* 93(11):1522–1529
- Roy PNS, Padhi A (2007) Multifractal analysis of earthquakes in the southeastern Iran-Bam region. *Pure Appl Geophys* 167:2271–2290
- Roy PNS, Ram A (2006) A correlation integral approach to the study of 26 January 2001 Bhuj earthquake, Gujarat India. *J Geodyn* 41:385–399
- Singh C, Singh A, Chadha RK (2009) Fractal and b-value mapping in Eastern Himalaya and Southern Tibet. *Bull Seismol Soc Am* 99(6):3529–3533
- Singh HN, Paudyal H, Shanker D, Panthi A, Kumar A, Singh VP (2010) Anomalous seismicity and earthquake forecast in Western Nepal Himalaya and its adjoining Indian Region. *Pure Appl Geophys* 167:667–684
- Sukmono S, Zen MT, Kadir WGA, Hendrajya L, Santoso D, Dubois J (1994) Fractal pattern of the Sumatra active fault system and its geodynamical implications. *J Geodyn* 22:1–9
- Sukmono S, Zen MT, Hendrajya L, Kadir WGA, Santoso D, Dubois J (1997) Fractal pattern of the Sumatra fault seismicity and its application to earthquake prediction. *Bull Seismol Soc Am* 87:1685–1690
- Sunmonu LA, Dimri VP (2000) Fractal geometry and seismicity of Koyna-Warna, India. *Pure Appl Geophys* 157:1393–1405
- Thingbaijam KKS, Nath SK, Yadav A, Raj A, Walling MY, Mohanty WK (2008) Recent seismicity in Northeast India and its adjoining region. *J Seismolog* 12:107–123
- Turcotte DL (1989) *Fractals in geology and geophysics*. *Pure Appl Geophys* 131:171–196
- Turcotte DL (1997) *Fractals and chaos in geology and geophysics*, 2nd edn. Cambridge University Press, New York, p 398